Study of the stability of a high-power PV conversion chain for isolated site supply

Edjadessamam Akoro[1*], *Yao Bokovi*[1], *Akueté Pierre Agbessi*[1], and *Gnakou Mazama Ateyo*[1]

[1]CERME (Centre d'Excellence Régional pour la Maîtrise de l'Electricité/ Laboratory of Research in Engineering Sciences (LARSI), Université de Lomé, Lomé, Togo

Abstract. The aim of this paper is to design and study the stability of a 500 kW PV string connected to a DC-AC load. To achieve this, a MPPT method based on a hybrid Artificial Neural Network (ANN)-Synergistic Control Algorithm (SCA) already developed in the literature will be used to find the system's maximum power point. This control will enable the PV generator to deliver maximum energy. Next, the power control approach will be developed to control the inverter, and the stability of the overall system will be studied.

Keywords: photovoltaic (PV), artificial neural network, maximum power point (MPPT), Synergic controller algorithm, stability.

1 Introduction

Photovoltaic solar energy comes from the direct conversion of a portion of the sun's rays into electrical energy. This energy conversion takes place via a so-called photovoltaic (PV) cell, based on a physical phenomenon known as the photovoltaic effect, which produces an electromotive force when the surface of the cell is exposed to light. These solar cells are assembled to form solar modules, which in turn are combined to form photovoltaic fields [1]. Several authors, including (C. Cabal, 2008) [2] and (Fatou Ndiaye et al, 2015) [3], have shown that the I-V and P-V characteristics of the PV field of a PV production string depend on climatic parameters such as irradiance and temperature. However, these parameters are not stable and can vary abruptly, which could lead to problems transferring the maximum power from the PV field to the rest of the system. The integration of PV systems into the electricity grid or decentralized systems are becoming the most important applications for solar PV today. This trend is growing because of the many advantages of using renewable energy sources in decentralized power generation systems [4],[5]. However, these applications give rise to potential problems related to power quality (low power factor, harmonic distortion, poor control, etc.), and the non-perfect coupling between the PV

* Corresponding author: justinakoro@gmail.com

generator and the power electronics matching stage [2], making the system unstable. As a result, the entire PV production chain needs to be optimized. It is within this framework that the work in this paper is situated.

The document is structured into four main sections. The first part introduces the paper. The second section focuses on the modeling of DC part. The third section deal with the three-phase inverter and PQ control modeling. Finally, the fourth section illustrates the simulation results and discussions.

2 DC part modelling

This part concerns the search for the maximum power point of the PV field. For this, we use the results of a hybrid ANN-SCA approach between the artificial neural network method (ANN) and the synergistic control algorithm (SCA: Synergetic Control Algorithm) which was the subject of one of our publications in [6]. This approach consists in automatically generating the optimal duty cycle to seek the maximum power based on the instantaneous state of the climatic parameters. It is shown in Fig. 1. The principle is as follows: the ANN algorithm estimates the optimal voltage (V_{ref}) and current (I_{ref}) from the PV generator to the MPP, using irradiation (I) and temperature (T) as inputs. We assume that the input capacitor current Cin is negligible (I_{Cin}≈0) so I_{PV}≈I_L. Next, the SCA algorithm ensures that the inductor current is equal to the optimum current delivered by the GPV ($I_{ref} \approx I_L$) and V_0 the output voltage of the DC-DC converter is substantially equal to some reference value V_{0ref} (V_0≈V_{0ref}). From these values, the optimum duty cycle for driving the converter is calculated.

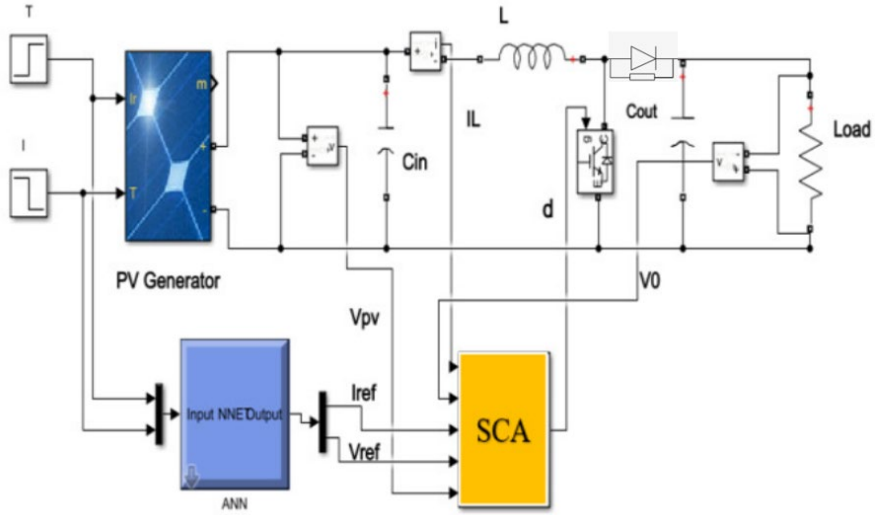

Fig. 1. Proposed schematic system.

The characteristics of the 500 kW PV generator designed in [6] are shown in Table 1.

Table 1. Characteristics of the 500 KW PV array

Technical data	**Values**
MPP voltage (Vmpp)	350 V
MPP current (Impp)	1436 A
No-load voltage (Vdc)	441 V
Short-circuit current (Isc)	1536 .2 A
V_{DC}	658 V

3 Three-phase inverter and PQ control modeling

3.1 Inverter modeling

A typical three-phase inverter circuit with an LC filter and a load [7] is shown in Fig.2. It consists of the photovoltaic (PV) system, symbolized here by the DC stage equipped with the hybrid ANN-SCA maximum power point search control, a three-phase inverter and finally an LC filter to reduce harmonic distortion [8].

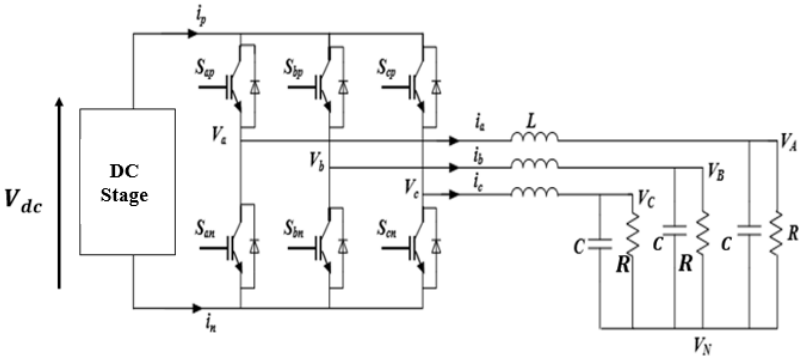

Fig.2. Three-phase voltage source inverter

The dynamic equations of a three-phase inverter with voltage source can be written as follows:

$$\frac{d}{dt}\begin{bmatrix} i_a \\ i_b \\ i_c \end{bmatrix} = \frac{1}{L}\begin{bmatrix} d_a \\ d_b \\ d_c \end{bmatrix} V_{dc} - \frac{1}{L}\begin{bmatrix} V_{AN} \\ V_{BN} \\ V_{CN} \end{bmatrix} - \frac{1}{L} \quad (1)$$

$$\frac{d}{dt}\begin{bmatrix} V_{AN} \\ V_{BN} \\ V_{CN} \end{bmatrix} = \frac{1}{C}\begin{bmatrix} i_a \\ i_b \\ i_c \end{bmatrix} - \frac{1}{RC}\begin{bmatrix} V_{AN} \\ V_{BN} \\ V_{CN} \end{bmatrix} \quad (2)$$

Where $[d_a, d_b, d_c]^{T}$ = u(t) is the control vector, containing the PWM module's duty cycle.

After transforming the variables from fixed coordinates Xabc to rotating coordinates Xdqz, known as the Park transformation [9,10], and considering that the Z component is zero and the power source is ideal, the space state equation of the small-signal model can be described by: (3) et (4) [7],[11] [12],[13]:

$$\frac{d}{dt}\begin{bmatrix}\widetilde{i_d}\\ \widetilde{i_q}\end{bmatrix} = \frac{1}{L}\begin{bmatrix}\widetilde{d_d}\\ \widetilde{d_q}\end{bmatrix} V_{dc} - \frac{1}{L}\begin{bmatrix}\widetilde{v_d}\\ \widetilde{v_q}\end{bmatrix} - \begin{bmatrix}0 & -\omega\\ \omega & 0\end{bmatrix}.\begin{bmatrix}\widetilde{i_d}\\ \widetilde{i_q}\end{bmatrix} \quad (3)$$

$$\frac{d}{dt}\begin{bmatrix}\widetilde{v_d}\\ \widetilde{v_q}\end{bmatrix} = \frac{1}{C}\begin{bmatrix}\widetilde{i_d}\\ \widetilde{i_q}\end{bmatrix} - \begin{bmatrix}\frac{1}{RC} & -\omega\\ \omega & \frac{1}{RC}\end{bmatrix}\begin{bmatrix}\widetilde{v_d}\\ \widetilde{v_q}\end{bmatrix} \quad (4)$$

With ω the pulse
These equations of state can be written in matrix form:

$$\dot{\tilde{x}} = A\tilde{x} + B\tilde{u} \quad (5)$$
$$\tilde{y} = C\tilde{x} \quad (6)$$

Where, $\tilde{x}$ is the state vector and $\tilde{y}$ the output vector. This gives:

$$\tilde{x} = \begin{bmatrix}\widetilde{v_d} & \widetilde{v_q} & \widetilde{i_d} & \widetilde{i_q}\end{bmatrix}^T \quad (7)$$
$$\tilde{u} = \begin{bmatrix}\widetilde{d_d} & \widetilde{d_q}\end{bmatrix}^T \quad (8)$$
$$C = I \quad (9)$$

The state (A), control (B) and care (C) matrices are defined respectively by:

$$A = \begin{bmatrix}-\frac{1}{RC} & \omega & \frac{1}{C} & 0\\ -\omega & -\frac{1}{RC} & 0 & \omega\\ \frac{-1}{L} & 0 & 0 & \omega\\ 0 & \frac{-1}{L} & -\omega & 0\end{bmatrix} \quad (10)$$

$$B = \begin{bmatrix}0 & 0\\ 0 & 0\\ \frac{V_{dc}}{L} & 0\\ 0 & \frac{V_{dc}}{L}\end{bmatrix} \quad (11)$$

$$C = [1\,0\,0\,0; 0\,1\,0\,0] \quad (12)$$

3.2 Inverter control

For inverter control, the PQ method has been used [79]. The principle consists in controlling the active and reactive power at the inverter output by the instantaneous values of the inverter output current components idref and iqref, respectively. The control is subdivided into two loops: an internal loop that independently regulates the inverter output currents (id and iq) in the rotating reference frame, and an external loop that produces the reference currents to regulate active (P) and reactive (Q) power (Fig.3).

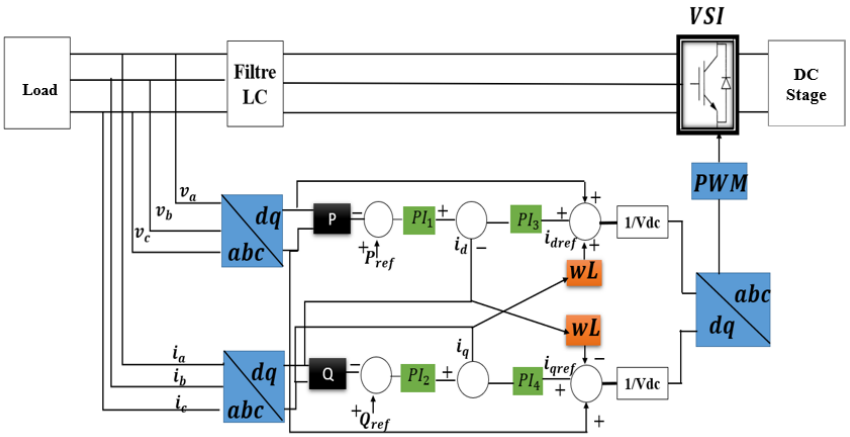

Fig .3. PQ control of three-phase inverter

PI_1, PI_2, PI_3, PI_4 are PI (proportional, integral) controllers [14].

Using Fig.3, the complete model of the closed-loop system [15],[16], is determined by equations (13) and (14):

$$\mathrm{pZ(p)} = (\mathrm{A_1} + \mathrm{B_1H_1})\mathrm{Z(p)} + \mathrm{B_2R(p)} \qquad (13)$$

$$\frac{\mathrm{Z(p)}}{\mathrm{R(p)}} = (\mathrm{pI} - \mathrm{A_1} - \mathrm{B_1H_1})^{-1}.\mathrm{B_2} \qquad (14)$$

Where $R(p) = \left[\left(\tilde{P}\tilde{Q}\right)_{ref}\right](p)$ et $B_2 = (B_1 J + B_r)$ et p the Laplace variable.

With :

$$H_1 = \frac{1}{V_{dc}}\begin{bmatrix} 1-\frac{3}{2}K_{idp}K_{Pp}I_d & -\frac{3}{2}K_{idp}K_{Pp}I_q & -\left(\frac{3}{2}K_{idp}K_{Pp}V_d + K_{idp}\right) & -\left(\frac{3}{2}K_{idp}K_{Pp}V_q + \omega L\right) & K_{idi} & 0 \\ 1-\frac{3}{2}K_{idp}K_{Pp}I_d & \left(1-\frac{3}{2}K_{iqp}K_{Qp}I_d\right) & -\left(\omega L - \frac{3}{2}K_{iqp}K_{Qp}V_q\right) & \left(\frac{3}{2}K_{iqp}K_{Qp}V_d - K_{iqp}\right) & 0 & K_{iqi} \end{bmatrix}$$

$$J = \frac{1}{V_{dc}}\begin{bmatrix} K_{idp}K_{Pp} & 0 \\ 0 & K_{iqp}K_{Qp} \end{bmatrix}$$

$$A_1 = \begin{bmatrix} -\frac{1}{RC} & \omega & \frac{1}{C} & 0 & 0 & 0 \\ -\omega & -\frac{1}{RC} & 0 & \omega & 0 & 0 \\ \frac{-1}{L} & 0 & 0 & \omega & 0 & 0 \\ 0 & \frac{-1}{L} & -\omega & 0 & 0 & 0 \\ -\frac{3}{2}K_{Pp}I_d & -\frac{3}{2}K_{Pp}I_q & -\left(\frac{3}{2}K_{Pp}V_d + 1\right) & -\frac{3}{2}K_{Pp}V_q & 0 & 0 \\ \frac{3}{2}K_{Qp}I_q & -\frac{3}{2}K_{Qp}I_d & -\frac{3}{2}K_{Qp}V_q & \left(\frac{3}{2}K_{Qp}V_d - 1\right) & 0 & 0 \end{bmatrix}$$

$$B_1 = \begin{bmatrix} 0 & 0 \\ 0 & 0 \\ \frac{V_{dc}}{L} & 0 \\ 0 & \frac{V_{dc}}{L} \\ 0 & 0 \\ 0 & 0 \end{bmatrix} \qquad B_r = \begin{bmatrix} 0 & 0 \\ 0 & 0 \\ 0 & 0 \\ 0 & 0 \\ K_{pp} & 0 \\ 0 & K_{Qp} \end{bmatrix}$$

A_1 and B_1 are the state matrices of the closed-loop system input. To find the optimum parameters for the 4 PI controllers, system stability was studied using the closed-loop transfer function (14).

After analyzing the behavior of the inverter's active and reactive power for different PI parameter values in matlab, we selected the values (Table 2) that would ensure high active and reactive power stability.

Table 2: PI controller parameters

PI controller parameters		
Kpp	Kqp	Kidp
1	-0,1	0.001
Kidi	Kiqp	Kiqi
1	0	10

4 Results and discussions

In this section, we'll be looking at the behavior of the various parts of the PV production chain, in particular the DC-DC and DC-AC matching stages. the entire system was simulated using Matlab/Simulink software.

4.1 Behavior of the DC-DC stage

The DC-DC stage was simulated at several irradiation and temperature levels (Fig. 4 and 5). The aim was to assess the behavior of the stage under sudden variations in climatic parameters. Curves 6, 7, 8 and 9 show the evolution of signals at the output of the 500 kW PV array and the boost converter.

Between 0 and 1s, irradiation and temperature are at standard conditions, i.e. 1000 W/m^2 and 25º C respectively. During this period, the PV field voltage Vmpp is 350 V and the boost converter output voltage is around 658 V (Fig.6). In terms of power, the PV field output Pmpp is around 500 kW (Fig.7). The Impp current is 1436 A and the current at the output of the boost converter is around 760 A (Fig.8). These values are in line with the PV array sizing

(Table 3). Over the remainder of the simulation time, we can also see that the ANN-SCA method adapts well to different variations in climatic parameters and remains accurate.

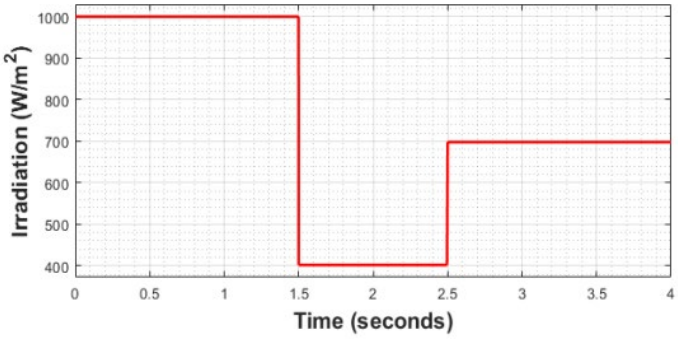

Fig. 4. Irradiation level variations

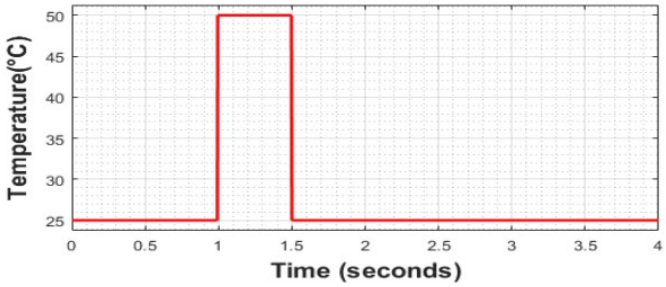

Fig. 5. Temperature level variations.

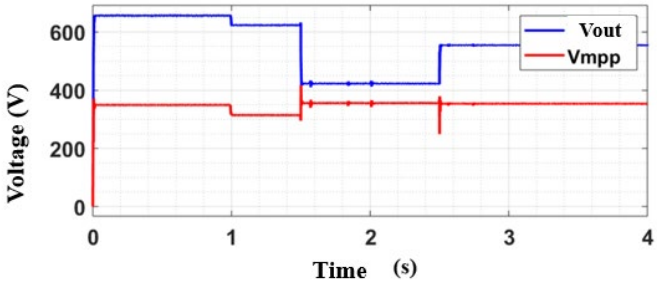

Fig.6. GPV and boost converter output voltage

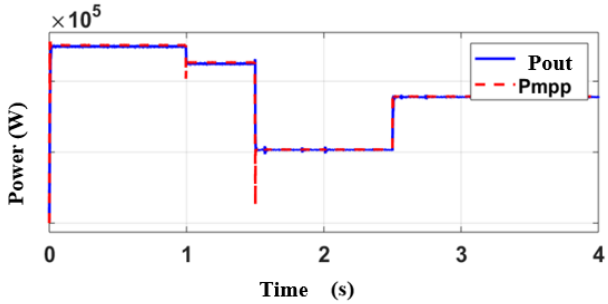

Fig. 7. GPV and boost converter output power

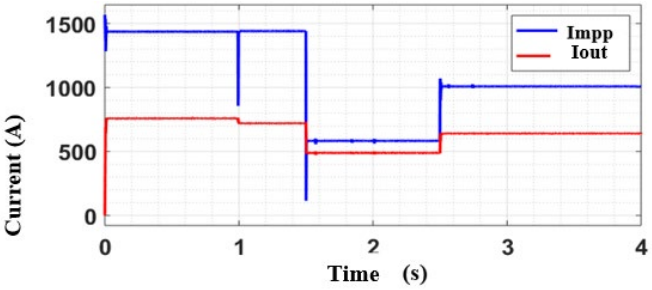

Fig.8. GPV and boost converter output current

4.2 Stability and behavior of the DC-AC stage

After studying the stability of the inverter + load filter block and finding the optimum parameters for the PI controllers, the output signals from these units were visualized for assessment. First, the reference active power is set to 500 kW and the reactive power is set to 0 VAR, i.e. the power factor is 1. Then, to check the controller's performance in following the power variation due to climatic parameters that can vary abruptly, at 0.1s the reference active power is reduced to 250 kW, while the reactive power is set to 100 kVAR, i.e. the power factor is 0.8. The curves in Fig.9 show that active and reactive power follow their references well, even in the event of abrupt variations in the latter, demonstrating that inverter control is working well.

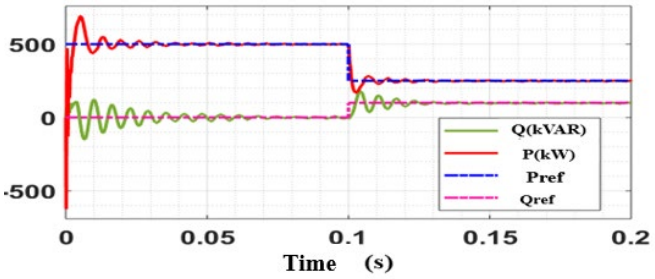

Fig.9. Trend of reactive and active power at inverter output

According to Figs.10 and 11, the 311 V voltage value corresponds to the amplitude of a line voltage (220*√2), while the 1074 A current is in agreement with the calculated values.

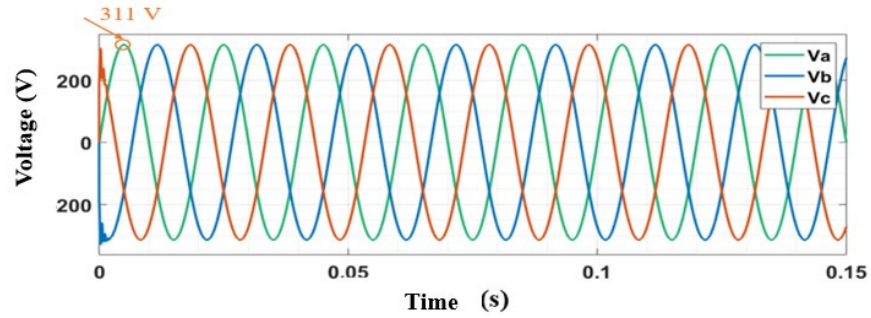

Fig.10. Evolution of inverter output voltage

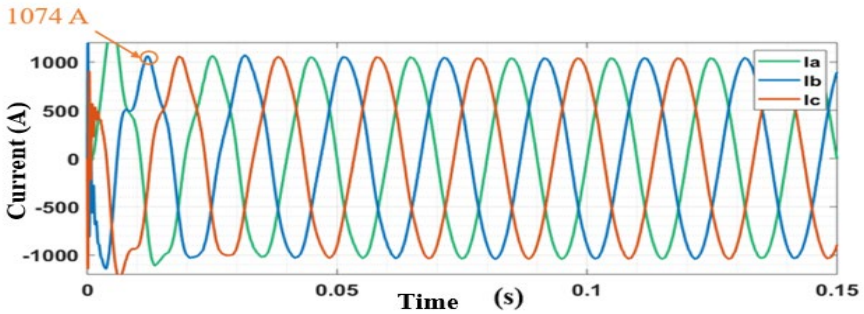

Fig.11. Load current trend

4.3 Visualization of harmonic distortion rates (THD)

Total Harmonic Distortion (THD) is an indicator of the quality of a device's output signals. It is obtained by comparing the output signals of the input inverter. According to IEEE standard 929-2000, the overall permissible harmonic content in voltage and current is set at 5% [17], [18]. To better appreciate the quality of the signals delivered by the inverter to the load, we visualized the THD of the voltage and current. According to Figs.12 and 13, the harmonic distortion rates of the inverter's output voltage and current are 1.12% and 2.46% respectively. These rates are lower than the 5% recommended by IEEE standard 929-2000. The signals are therefore of good quality.

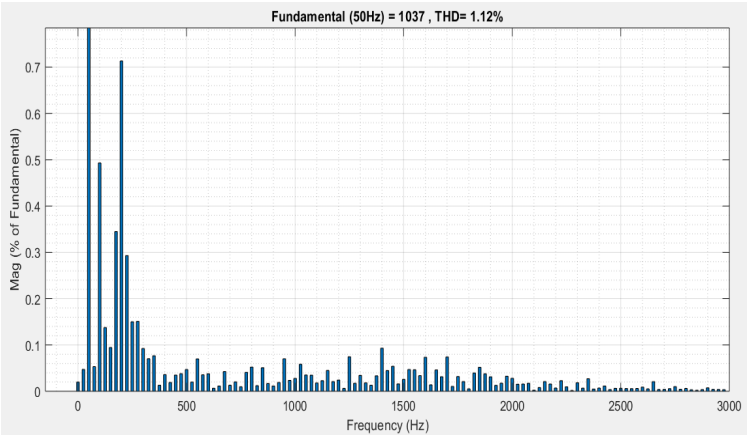

Fig. 12. Harmonic waveform of inverter output voltage

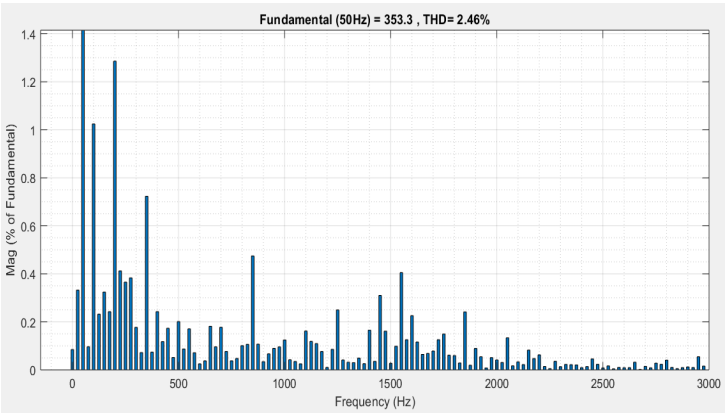

Figure 13: Harmonic waveform of inverter output current

5 Conclusion

In this paper, the 500 kW PV production line has been designed. An approach based on a hybridization of the ANN and SCA methods was used. PQ control was developed to control the inverter. A priori, the photovoltaic generation system performs well under different solar irradiation and PV field temperature conditions. At the same time, it maintains stability and extracts maximum power from the GPV. The harmonic distortion rate of the inverter voltage is 1.12% and that of the load current is 2.46%, well below the 5% recommended by the IEEE standard. All in all, this system has been designed to optimize the entire photovoltaic conversion chain.

References

1. Flansanier, « Photovoltaic Engineering Handbook». IOP Publishing Ltd. 1980. ISBN 0 85274-311-4.
2. C. Cabal, « Optimisation énergétique de l'étage d'adaptation électronique dédié à la conversion photovoltaïque », Université de Toulouse III Paul Sabatier., p. 188, 2008.
3. F. Ndiaye, M. Sene, M. Beye, et A. S. H. Maiga, « Effects of Climatic Conditions on a Polycrystalline Photovoltaic Module in Niger », ILCPA, vol. 55, p. 59-65, juill. 2015, doi: 10.18052/www.scipress.com/ILCPA.55.59.
4. A. Refaat, A. Kalas, A. Daoud, and F. Bendary, 'A Control Methodology of Three Phase Grid Connected PV System', in Clemson University Power Systems Conference (PSC 2013), 2013
5. M. Liberos, R. González-Medina, G. Garcerá, et E. Figueres, « Modelling and Control of Parallel-Connected Transformerless Inverters for Large Photovoltaic Farms », Energies, vol. 10, no 8, p. 1242, août 2017, doi: 10.3390/en10081242.
6. Akoro, E., Tevi, G. J., Faye, M. E., Doumbia, M. L. and Maiga, A. S. (2020). Artificial Neural Network Photovoltaic Generator Maximum Power Point Tracking Method using Synergetic Control Algorithm. International Journal on Emerging Technologies, 11(2): 590–594.
7. Y. Zhang, Z. Jiang, and X. Yu, «Small-signal modeling and analysis of parallelconnected voltage source inverters» in Power Electronics and Motion Control Conf., 2009. IPEMC'09. IEEE 6th Int., 2009, p. 377–383.
8. A. Beddar, I. Abadlia, F. Abdoune, L. Hassaine, M. Rida Bengourina :Investigation and implementation of a nonlinear decoupled power control for a single-phase grid connected power inverter via an LCL filter, Journal of Engineering Research 11 (2023) 100010.
9. N. Hanisah Baharudin, T. Muhammad Nizar Tunku Mansur, F. Abdul Hamid, R. Ali, et M. Irwanto Misrun, « Topologies of DC-DC Converter in Solar PV Applications », IJEECS, vol. 8, no 2, p. 368, nov. 2017, doi: 10.11591/ijeecs.v8.i2.pp368-374.
10. K. C. A. de Souza, M. R. de Castro, et F. Antunes, « A DC/AC converter for single-phase grid-connected photovoltaic systems », in IEEE 2002 28th Annual Conference of the Industrial Electronics Society. IECON 02, Sevilla, Spain, 2002, p. 3268-3273, doi: 10.1109/IECON.2002.1182922.

11. Ye Z., «Modeling and Control of Parallel Three-Phase PWM Converters», PhD Dissertation, Virginia Tech, Sept 2000
12. A. Khalil, K. A. Alfaitori, et A. Elbarsha, « Stability analysis of parallel-inverters in microgrid », in 2014 20th International Conference on Automation and Computing, sept. 2014, p. 110-115, doi: 10.1109/IConAC.2014.6935471.
13. Khaled Ateea Elfitory, « Modeling and Control of Parallel Three-Phase Voltage Source Inverters with Different D.C Sources », University of Benghazi, Faculty of Engineering Electrical and Electronic Engineering, Department Postgraduate Studies, 2014.
14. J. C. Basilio et S. R. Matos, « Design of PI and PID controllers with transient performance specification », IEEE Trans. Educ., vol. 45, no 4, p. 364-370, nov. 2002, doi: 10.1109/TE.2002.804399.
15. Wang Jianhong & Ricardo A. Ramirez-Mendoza, «The practical analysis for closed-loop system identification », Cogent Engineering (2020), 7: 1796895.
16. Radouan Gouaamar1*, Seddik Bri, and Zineb Mekrini «Comparative Analysis between Proportional-Integral and Artificial Neural Network Control of a Grid-Connected PV System»E3S Web of Conferences 469, 00003 (2023) ICEGC'2023
17. « IEEE Recommended Practice for Utility Interface of Photovoltaic (PV) Systems », IEEE. doi: 10.1109/IEEESTD.2000.91304.
18. Ioan Viorel Banu, Fadila Barkat, Marcel Istrate, Josep M. Guerrero, George Culea, Petru Livinti, Justina G. Motas, Bogdan Neagu, Dragos Andrioaia, «Passive anti-Islanding protection for Three-Phase Grid-Connected photovoltaic power systems », International Journal of Electrical Power & Energy Systems,Volume 148, 2023, ISSN 0142-0615,